Chemical Engineering Journal 158 (2010) 451–457

Contents lists available at ScienceDirect

Chemical Engineering Journal

journal homepage: www.elsevier.com/locate/cej

Equilibrium and kinetics of adsorption of fluoride onto zirconium impregnated cashew nut shell carbon

G. Alagumuthu*, M. Rajan[1]

PG & Research Centre of Chemistry, Sri Paramakalyani College, Sivasailam Road, Alwarkurichi 627412, Ambasamudram (TK), Tirunelveli, Tamilnadu, India

ARTICLE INFO

Article history:
Received 20 November 2009
Received in revised form 8 January 2010
Accepted 11 January 2010

Keywords:
Adsorption
Cashew nut shell
Fluoride
Isotherm
Kinetics

ABSTRACT

Zirconium impregnated cashew nut shell carbon was studied to assess its capacity for the adsorption of fluoride from aqueous solutions. The dependence of the adsorption of fluoride on the pH of the solution has been studied to achieve the optimum pH value and a better understanding of the adsorption mechanism. The influence of addition of the co-existing ions on the adsorption of fluoride was also studied. Adsorption isotherms have been modeled by Langmuir, Freundlich and Redlich–Peterson equations and their constants were determined. Pseudo-first- and second-order equations were used to describe the adsorption rate of fluoride and adsorption rate constant was calculated. A mechanism involving three stages, viz.; external surface adsorption, intra-particle diffusion and final equilibrium has been proposed for the adsorption of fluoride onto adsorbent material. Thermodynamic parameters such as ΔG°, ΔH° and ΔS° were calculated in order to understand the nature of sorption. Field studies were carried out with the fluoride containing water sample collected from a fluoride-endemic area in order to test the suitability of the sorbent at field conditions.

1. Introduction

Millions of people particularly in developing countries are suffering from fluorosis due to high fluoride concentrations in their drinking water [1]. Fluorosis is characterized by discolored, blackened, molted (or) chalky white teeth. In India this problem is common in places such as Andhra Pradesh, Tamilnadu, Karnataka, Kerala, Rajasthan, Gujarat, Uttar Pradesh, Punjab, Orissa and Jammu and Kashmir [2]. Free fluoride level in drinking water was identified at 3.02 ppm in Kadayam block of Tamilnadu [3]. Fluoride survey in Nilakottai block of Tamilnadu showed a positive correlation between prevalence of dental fluorosis in children and levels of fluoride in portable water is 3.24 ppm [4]. The excess of fluoride (>1.5 ppm) has been removed by various methods.

Adsorption is one of the most efficient technologies for fluoride removal from drinking water when compared with other technologies such as reverse osmosis [5], nanofiltration [6], electro-dialysis [7,8] and Donnan dialysis [9]. Many natural and low cost materials such as nirmali seeds [10], adsorption by powered and granular red mud [11,12], zirconium impregnated coconut shell carbon [13] and clays [14] have been used as adsorbents for fluoride removal from water. Studies on various sources of activated carbon have been done by many researchers [15]. Activated carbons and modified activated carbon are potential adsorbents because of their strong affinity for fluoride [13]. The rare earth metals are usually expensive, which restricts their use in the treatment of drinking water. Because of the high electro-negativity and small ionic size of the fluoride ion, it has a strong affinity towards multivalent metal ions including Al (III), Fe (III) and Zr (IV) [16]. In this study the cashew nut shell is carbonized and is impregnated with zirconium oxy chloride.

The present work is expected to explore the feasibility of cashew nut shell carbon in the removal of fluoride from aqueous solutions. Cashew nut is one of the commercialized products of the cashew tree and the cashew nut shell is the waste product of cashew nut. Cashew nut shell contains various potassium and magnesium compounds [17]. The removal of fluoride from aqueous solution by cashew nut shell carbon and zirconium impregnated cashew nut shell carbon were studied and discussed.

2. Materials and methods

2.1. Preparation of activated carbon

Activated carbon was prepared as per the procedure [18] from cashew nut shell (*Anacardium occidentale*); about 100 g of the crushed cashew nut shell was kept for 3 h in a low temperature muffle furnace at 573–673 K. The carbonized material was taken out of the muffle furnace, cooled, powered and kept in a beaker

* Corresponding author. Tel.: +91 09790594279; fax: +91 04634283226.
E-mail addresses: alagupathi@yahoo.co.in (G. Alagumuthu), rajanm153@gmail.com (M. Rajan).
[1] Tel.: +91 09095325573; fax: +91 04634283226.

1385-8947/$ – see front matter © 2010 Elsevier B.V. All rights reserved.
doi:10.1016/j.cej.2010.01.017

and 200 ml of concentrated sulphuric acid was gradually added to it, contents were stirred continuously to ensure thorough mixing. The activated carbon was then cooled and left overnight and washed free of acid and dried at 383 K for 2 h, then sieved using various mesh size. Subsequently the activated carbon was further immersed in 2N NaOH solution and washed free of alkali, providing the desired adsorbent for impregnation.

Zirconium ion impregnation was carried out by adding 5% $ZrOCl_2$ solution with activated carbon (solution/solid ratio = 2:1) and the mixture being kept for 3 days at room temperature (298 K). The impregnated carbon was then filtered, rinsed to confirm the effluent free from zirconium, dried in an oven at 380 K and subsequently used for defluoridation studies. The zirconium concentration in the effluent was determined using ammonia and alizarin red S (ARS) [19]. Zirconium is generally non-toxic as an element or in compound and the oral toxicity is low. OSHA standard for pulmonary exposure specify a TVL of 5 mg zirconium per m^3. As per the solubility product of zirconyl oxy chloride ($K_{sp} = 6.3 \times 10^{-49}$), the solubility of it is 26.7×10^{-15} g/L. Hence the amount of zirconium ion concentration in the effluent is well below the safe limit. As solubility factor calculations could be at variance with experimental results, a quantitative analysis was further carried out to determine the concentration Zr^{4+} ion in the effluent and in the treated water samples by using spectrophotometric studies at a wavelength of 520 nm, as it is sensitive towards the small change of Zr^{4+} concentration and operate in the dynamic range of 5–35 mg/L at pH 2.5. All the tested samples had the Zr^{4+} ion concentration less than 5.0 mg/L. The defluoridation capacity of ZICNSC was investigated by pursuing the batch equilibrium and kinetic experiments.

The reagents used in this present study are of analytical grade. A fluoride ion stock solution (100 mg/L) was prepared and other fluoride test solutions were prepared by subsequent dilution of the stock solution. All the experiments were carried out at room temperature. Fluoride ion concentration was measured with a specific ion selective electrode by use of total ionic strength adjustment buffer (TISAB) solution to maintain pH 5–5.5 and to eliminate the interference effect of complexing ions [20]. The pH of the samples was also measured by Orion ion selective equipment. All other water quality parameters were analysed by using standard methods [21].

2.2. Sorption experiments

The sorption isotherm and kinetics experiments were performed by batch adsorption experiments and were carried out by mixing 1.5 mg of sorbent with 100 ml of sodium fluoride containing 3 mg/L as initial fluoride concentration. The mixture was agitated in a thermostatic shaker at a speed of 200 rpm at room temperature. The defluoridation studies were conducted for the optimization of various experimental conditions like contact time, pH, initial fluoride concentration and influence of co-ions with fixed dosage. Kinetic studies of sorbent were carried out in a temperature controlled mechanical shaker. The effect of different initial fluoride concentrations viz., 2, 4, 6, 8 and 10 mg/L at four different temperatures viz., 303, 313, 323 and 333 K on sorption rate were studied by keeping the mass of sorbent as 1.5 mg and volume of solution as 100 ml in neutral pH. The pH at zero point charge (pHzpc) of sorbent was measured using the pH drift method [22]. The pH of the solution was adjusted by using 0.01 mol/L sodium hydroxide or hydrochloric acid. Nitrogen was bubbled through the solution at 30 °C to remove the dissolved carbon dioxide. 50 mg of the adsorbent was added to 50 ml of the solution. After stabilization, the final pH was recorded. The graph of final pH versus initial pH was used to determine the zero point charge of the activated carbon.

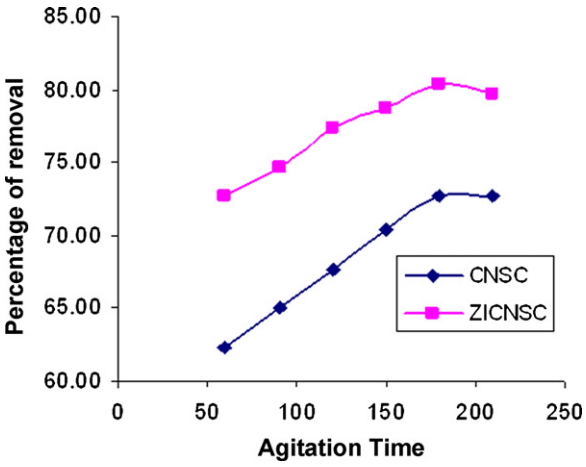

Fig. 1. Effect of contact time on fluoride adsorption.

2.3. Characterization of sorbents

The X-ray diffraction (XRD) pattern of the impregnated carbon was obtained using a Bruker AXS D8 Advance, Inst ID: OCPL/ARD/26-002 X-ray diffractometer. Fourier transform infrared spectra were recoded using Nicolet 6700, Thermo Electronic Corporation, USA made spectrophotometer. Computations were made using Microcal Origin (Version 6.0) software. The accuracy of fit is discussed using regression correlation coefficient (r) and chi-square analysis (SSE). The chi-square statistic test is basically the sum of the square of the difference between the experimental data and data obtained by calculating from the models, with each squared difference divided by the corresponding data obtained by calculating from the models. The equivalent mathematical statement is:

$$\chi^2 = \sum \frac{(q_e - q_e, m)^2}{q_e, m} \quad (1)$$

where q_e,m is equilibrium capacity obtained by calculating from the model (mg/g) and q_e is experimental data of the equilibrium capacity (mg/g).

3. Results and discussion

3.1. Effect of contact time

Fig. 1 illustrates the percentage of fluoride removal by CNSC and ZICNSC as a function of contact time in the range of 60–210 min at room temperature. The values are increasing linearly up to 180 min and thereafter it remained almost constant indicating the attainment of sorption equilibrium. Therefore 180 min was fixed as minimum contact time for the maximum defluoridation of the sorbent. The zirconium impregnated cashew nut shell carbon recorded a maximum percentage of fluoride removal 80.33% when compared with cashew nut shell carbon 72.67%.

3.2. Effect of particle size

The defluoridation experiments were conducted using CNSC with five different particle sizes viz. >53, 53–106, 106–212, 212–300 and 300–426 μm. As the adsorption process is a surface phenomenon, the defluoridation efficiency of the sample with 53 μm registered high defluoridation efficiency due to larger surface area. The percentages of fluoride removal by the sample with different particle sizes are studied. Hence the material with particle size of 53 μm has been chosen for further experiments. Higher per-

centage of adsorption by CNSC with smaller particle size is due to the availability of more specific surface area on the adsorbent surface. All the forthcoming discussion is based on the experimental result using this sample.

3.3. Influence of pH

The fluoride sorptive effect at different pH environments were also experimentally verified for CNSC and ZICNSC by varying the pH ranges from 3 to 12. At pH 3, the maximum percentage of fluoride removal by CNSC and ZICNSC was 83.67% and 87.00%, respectively. At higher pH values the fluoride removal by the sorbents was found to decrease. The same trend was also observed in *Morringa indica* based activated carbon [23]. The pH_{zpc} of CNSC (7.6) and ZICNSC (4.2) were determined. The maximum percentage of fluoride removal by the samples was observed at pH 3. It is due to the availability of more H^+ ions in the surface of the adsorbent leading to greater adsorption of the fluoride. Hence, fluoride adsorption increases at low pH levels as more of the surface sites are positively charged. The adsorption of fluoride onto the surface of the material is due to the development of positively charged surface sites. The CNSC was sudden decrease after pH 8.0 compared to the ZICNSC. The reduction in the percentage of adsorption of fluoride at higher pH level is due to the increasing electrostatic repulsion between negatively charged surface sites of the adsorbent and fluoride ions.

3.4. Assessment of influence of interfering co-ions

Defluoridation studies of ZICNSC were carried out in the presence of common ions like sulphate, chloride, bicarbonate, and nitrate, which are normally present in water were experimentally verified. The concentration of co-existing ions was varied from 50 to 500 mg/L with an initial fluoride concentration of 10 mg/L at neutral pH. It was inferred that there was no remarkable influence on the removal of fluoride in presence of Cl^-, SO_4^{2-} and nitrate. However the presence of bicarbonate ion resulted in the decrease of percentage from 80.33% to 60.23%. This may be due to the competition of bicarbonate ions with fluoride for sorption sites. Similar trend was reported while studying activated alumina as a sorbent for fluoride removal [24].

3.5. Adsorption isotherms

The sorption isotherm expresses the specific relation between the concentration of sorbate and its degree to accumulation onto sorbent surface at constant temperature. The fluoride sorption capacity of ZICNSC was evaluated using three different isotherms namely Langmuir [25], Freundlich [26] and Redlich–Peterson [27] isotherms.

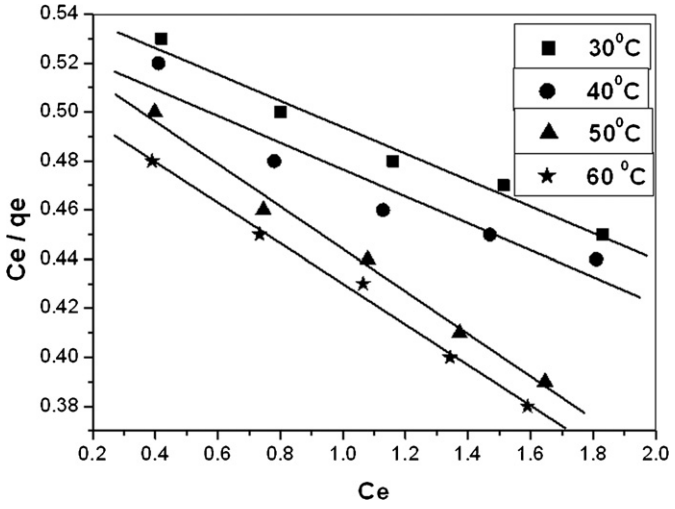

Fig. 2. Plot of the Langmuir isotherm for fluoride adsorption at pH 7.0 (±0.1) on ZICNSC. Experimental data points at 303, 313, 323 and 333 K.

The linear form of Langmuir isotherm is

$$\frac{C_e}{q_e} = \frac{1}{Qb} + \frac{C_e}{Q} \tag{2}$$

The Langmuir isotherm constants Q and b were calculated from the slope and intercept of the plot C_e/q_e vs. C_e shown in Fig. 2 and the results are listed in Table 1. The values of Q were found to increase with rise in temperature, which indicated sorption capacity increased with rise in temperature, which in turn suggested the mechanism of fluoride removal by the sorbent was mainly due to chemisorption. The higher r values indicated the applicability of Langmuir isotherm.

$$\ln\ q_e = \ln K_F + \left(\frac{1}{n}\right) \ln C_e \tag{3}$$

The values of Freundlich isotherm constants $1/n$ and K_F were calculated from the slope and intercept of the plot $\log q_e$ vs. $\log C_e$ (Fig. 3) and presented in Table 1. The values of $1/n$ lying between 0 and l and the n values lying in between 1 and 10 indicated that the conditions were favorable for adsorption and the r values indicated the applicability of Freundlich isotherm.

$$\log\left[\left(\frac{K_R C_e}{q_e}\right) - 1\right] = \beta \log C_e + \log(\alpha_R) \tag{4}$$

Table 1
Langmuir, Freundlich and Redlich isotherm parameters of fluoride sorption on ZICNSC.

Isotherm	Parameters	303 K	313 K	323 K	333 K
Langmuir isotherm	q_m (mg/g)	1.83	1.88	1.88	1.95
	b_L (L/g)	10.2	9.70	6.13	6.19
	R	0.988	0.955	0.995	0.997
	SSE	0.0048	0.0036	0.0097	0.0047
Freundlich isotherm	$1/n$	0.4923	0.4947	0.5652	0.5802
	n	2.0310	2.0212	1.7690	1.7234
	K_F (mg/g)	0.6132	0.6384	0.5773	0.2639
	r	0.981	0.975	0.983	0.987
	SSE	0.0537	0.0554	0.0647	0.0601
Redlich–Peterson isotherm	α_R	2.47	2.40	1.82	1.84
	β_R	0.119	0.108	0.183	0.197
	K_R	18.66	18.23	11.52	12.07
	r	0.991	0.999	0.977	0.948
	SSE	0.0045	0.0014	0.0116	0.0185

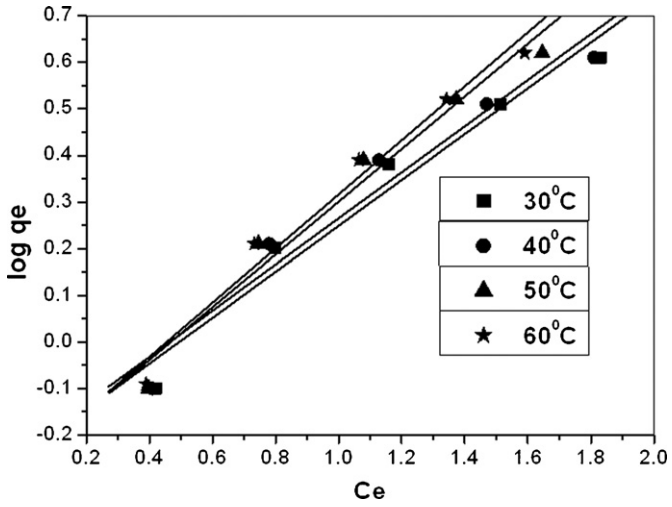

Fig. 3. Plot of the Freundlich isotherm for fluoride adsorption at pH 7.0 (±0.1) on ZICNSC. Experimental data points at 303, 313, 323 and 333 K.

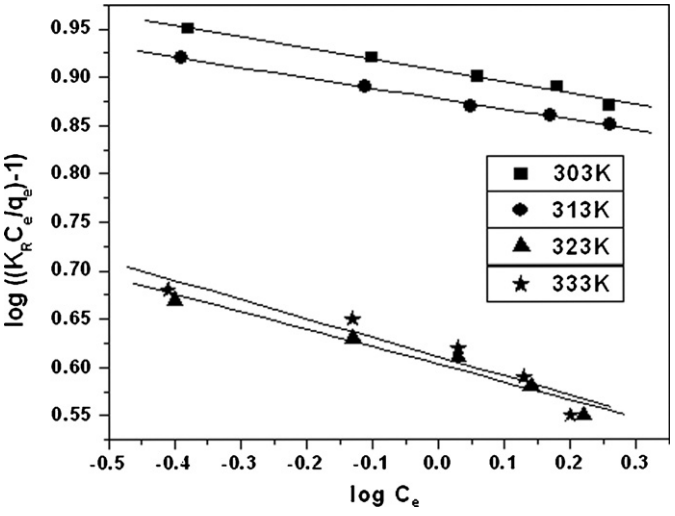

Fig. 4. Plot of the Redlich–Peterson isotherm for fluoride adsorption at pH 7.0 (±0.1) on ZICNSC. Experimental data points at 303, 313, 323 and 333 K.

where $K_R = Qb$ (L/g) i.e., Q and b are Langmuir monolayer capacity and energy of adsorption, respectively.

α_R = Exponent of R–P isotherm.

The values of Redlich–Peterson isotherm constant α and β were calculated from the slope and intercept of the plot $\log[(K_R C_e/q_e) - 1]$ vs. $\log(\alpha_R)$ (Fig. 4) and presented in Table 1. The feasibility of the isotherm was tested by calculating the dimensionless constant separation factor or equilibrium parameter, R_L [28]. The R_L values at different temperatures were calculated and given in Table 2. The R_L values lying between 0 and 1 indicated that the conditions were favorable for adsorption. The higher r values of Redlich–Peterson over Langmuir and Freundlich isotherm indicated the suitability of Redlich–Peterson isotherm than the Langmuir and Freundlich isotherm. This fact was further supported by low SSE values of Redlich–Peterson isotherm as shown in Table 1 [29].

Table 2
R_L values at different temperature.

S. no.	Concentration of fluoride mg/L	303 K	313 K	323 K	303 K
1	2	0.0467	0.0490	0.0754	0.0747
2	4	0.0239	0.0251	0.0391	0.0388
3	6	0.0160	0.0168	0.0264	0.0262
4	8	0.0121	0.0127	0.0199	0.0197
5	10	0.0097	0.0102	0.0160	0.0158

Table 3
Thermodynamic parameters of fluoride sorption on ZICNSC.

S. no	Thermodynamic parameters	Temperature (K)	ZICNSC
1	ΔG° (kJ mol^{-1})	303	−859.5
		313	−962.6
		323	−1065.6
		333	−1168.7
2	ΔH° (kJ mol^{-1})		0.717
3	ΔS° (J mol^{-1} K^{-1})		3.278

3.6. Thermodynamic investigations

The effect of temperature has a major influence in the sorption process and hence the sorption of ZICNSC was monitored at four different temperatures 303, 313, 323 and 333 K under the optimized condition and thermodynamic parameters viz., standard free energy change (ΔG°), standard enthalpy change (ΔH°) and standard entropy change (ΔS°) were calculated [30,31] and presented in Table 3. The negative values of ΔG° indicated the spontaneity of the sorption reaction. The positive values of ΔH° indicated the endothermic nature of the sorption process. The positive value of ΔS° showed the increasing randomness at the solid/liquid interface during sorption of fluoride. It also indicates the increased disorder in the system with changes in the hydration of adsorbing fluoride ions [32].

Table 4
Kinetic parameters of reaction-based and diffusion-based models with r and SSE values of ZICNSC.

Methods	Parameters	2 ppm	4 ppm	6 ppm	8 ppm	10 ppm
Pseudo-first-order	k_1 (min^{-1})	0.0148	0.0225	0.0199	0.0142	0.0101
	q_e (mg/g)	0.3908	0.4835	0.4951	0.4849	0.4889
	r	0.9608	0.9656	0.9656	0.9845	0.9963
	SSE	0.0013	0.0027	0.0016	7.7E−4	2.6E−4
Pseudo-second-order	k_2 (g/mg min)	−2628.79	−3889.72	−648.28	−336.37	0.00059
	h (g/mg min)	−3.4E−10	−5.7E−11	−3.4E−10	−1.6E−10	5.7E−05
	r	1.000	1.000	1.000	1.000	0.999
	SSE	2.3E−12	2.3E−12	2.3E−12	2.3E−12	2.3E−6
Intra-particle diffusion	k_p (min^{-1})	0.1091	0.2205	0.3331	0.33313	0.22052
	r	0.9263	0.9283	0.9284	0.9284	0.9283
	SSE	0.0198	0.0394	0.0596	0.05963	0.03949

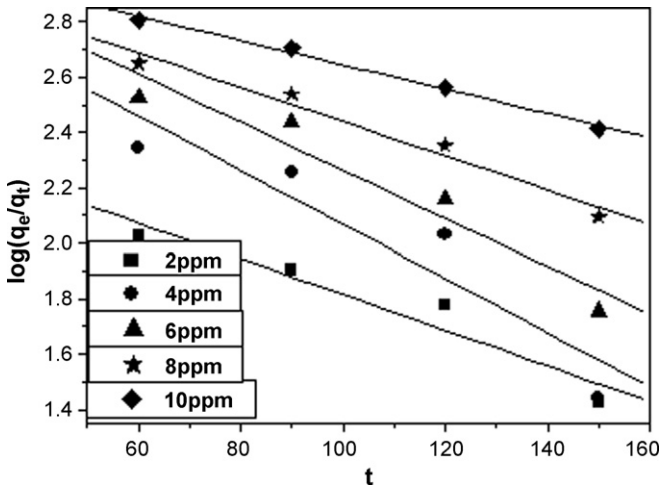

Fig. 5. Pseudo-first-order kinetic fit for fluoride adsorption onto ZICNSC at room temperature.

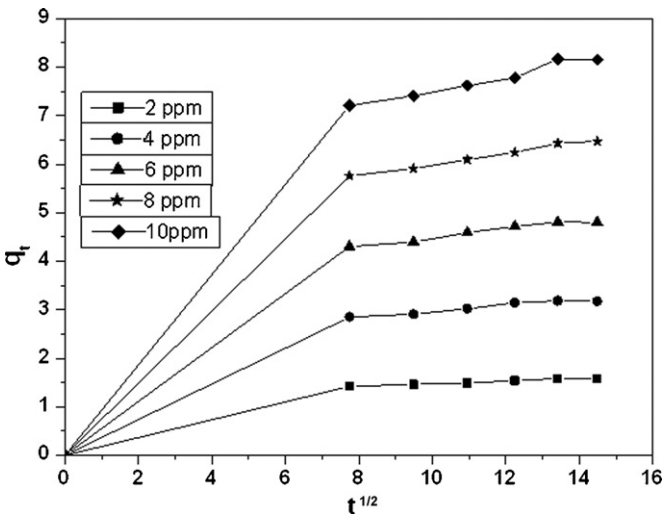

Fig. 7. Plot for constant intra-particle diffusion at different temperature.

3.7. Sorption kinetics

The two types of kinetic models viz., reaction-based and diffusion-based models were applied to test the fitness of experimental data [33].

3.7.1. Reaction-based models

The slope of the plot $\log(q_e - q_t)$ vs. t of pseudo-first-order equation [34] at different experimental conditions would give the values of the rate constant and were given in Table 4. The Lagergren plots of the reactions at the four temperatures are given in Fig. 5. The pseudo-second-order plot of t/q_t vs. t [35] resulted (Fig. 6) in a straight line with higher r values than the pseudo-first-order, which indicated the better applicability of pseudo-second-order model and the values were summarized in Table 4. The values of q_e increased with increase in initial fluoride concentration and it also increased with increase in temperature, which indicated the influence of chemisorption [36].

3.7.2. Diffusion-based models

In a solid–liquid sorption process the transfer of solute was characterized by particle diffusion [37,38] control. The intra-particle diffusion model was applied and the value of rate constants k_p was determined and given in Table 4. The trend was shown in Fig. 7.

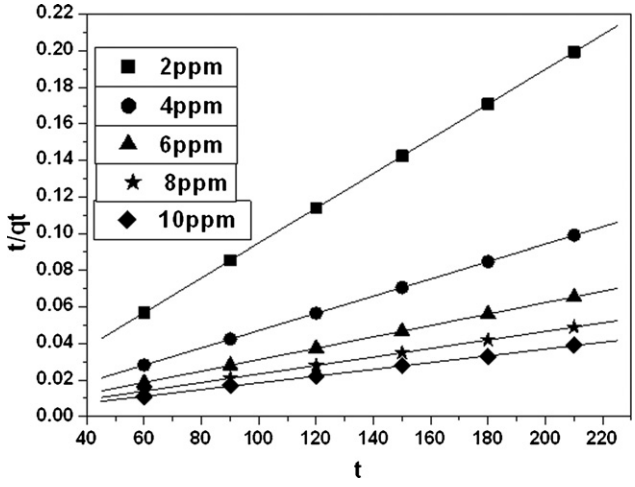

Fig. 6. Pseudo-second-order kinetic fit for fluoride adsorption onto ZICNSC at room temperature.

Higher r values indicated the possibility of sorption process being controlled by particle diffusion.

3.7.3. Fitness of sorption kinetic models

The kinetic models were evaluated for fitness of the sorption data by calculating the sum of errors squared (SSE). Lower values of SSE show a better fitness of the sorption data [33,38]. The SSE values of reaction-based and diffusion-based models were computed and also summarized in Table 4. It was identified that the pseudo-second-order was a better fit than pseudo-first-order and intra-particle diffusion model.

3.7.4. Mechanism of fluoride sorption

The fluoride removal by ZICNSC was governed by adsorption mechanism. The surface acquired positive charge at lower pH values and hence the fluoride sorption at this pH level was mainly due to electrostatic attraction between the positive charged surface and negatively charged fluoride ions and chemisorption dominated. As the pH is increased slowly, the surface acquired negative charges, physisorption dominated and hence the percentage removal of fluoride was decreased. The slight enhancement of fluoride removal by ZICNSC over CNSC may be due to sorption by zirconium, adsorption by physical forces and fluoride ion, a Lewis base, coordinates strongly with the zirconium species adsorbed on CNSC, which are Lewis acid sites.

$$ZrOCl_2{\cdot}8H_2O + H_2O \Leftrightarrow ZrOOHCl + Cl^- \quad (5)$$

$$ZrOOHCl(adsorbedonCNSC) + 2F^- - \Leftrightarrow ZrOF_2 + OH^- + Cl^- \quad (6)$$

The chemisorption mechanism of fluoride uptake, involves an exchange of the chloride and the hydroxide of the ZrO(OH)Cl species adsorbed on CNSC by fluorides, leading to the formation of $ZrOF_2$ [13]. The fluoride adsorption capacity of ZICNSC was compared with those of other commonly used fluoride adsorbent for 100 ml of 10 mg/L fluoride standard test solution with a ZICNSC adsorbent dose of 1.5 mg/100 ml and 108 min agitation time given in Table 5.

3.8. Desorption and reuse potential

Any adsorbent is economically viable if the adsorbent can be regenerated and reused in many cycles of operation. For checking the desorption capacity of the sorbent, the material was subjected to an adsorption at an initial fluoride concentration of 3 mg/L. The exhausted ZICNSC was regenerated using HCl and NaOH. NaOH

Table 5
Comparative study of fluoride adsorption onto various adsorbent at 303 K.

S. no.	Adsorbent	Fluoride adsorption percentage	
		pH = 4	pH = 7
1.	ZICNSC	90.4	81.7
2.	Alumina	59.6	41.2
3.	Phosphorus free carbon	27.8	15.4
4.	Chitin	14.8	6.2

Table 6
Field trial results of ZICNSC.

Water quality parameters	Before treatment	After treatment
F^- (mg/L)	2.89	0.56
pH	8.3	7.2
EC (mmho/cm^2)	3.16	1.44
Cl^- (mg/L)	650	282
Total hardness (mg/L)	589	241
Total alkalanity (mg/L)	560	268

is better regenerated than HCl. The concentrations were ranging from 0% to 10%. At 2.5% NaOH concentration, ZICNSC had desorbed almost 96.2% of fluoride. To test the adsorption potential of regenerated ZICNSC, two more cycles of adsorption–desorption studies were carried out by maintaining the initial conditions of the same. In third cycle, the adsorbent capacity has shown 28.00%. However, in the fourth cycle, adsorption capacity was observed as 5%. More tests have to be conducted to determine the exact life cycle of the adsorbent.

3.9. Field study

The defluoridation efficiency of both ZICNSC and CNSC in the field level was compared with the sample collected from a near by fluoride-endemic villages and the results are presented in Table 6. It has been observed that all the water quality parameters show marked improvement.

3.10. Instrumental studies

For understanding the nature of fluoride sorption X-ray and FTIR studies were performed using the raw and treated adsorbents. Powder X-ray diffraction was carried out on the raw and fluoride treated ZICNSC samples. The XRD patterns for treated adsorbents showed significant changes. The XRD data of the treated ZICNSC provided evidence of slight modification over the crystal cleavages. The intensity of the peak due to the *hkl* plane 0 1 0 of the monoclinic crystal system of ZICNSC disappeared after the fluoride adsorption on its surface. This is possible due to the lattice dislocation in the crystal system. The X-ray diffraction patterns of raw and fluoride treated material are given in Figs. 8 and 9. This shows the strong adsorption of fluoride on the surface of the adsorbent. Adsorption of fluoride has also resulted in several changes like the disappearance of some bands, shifts and decrease in the percentage of transmittance in the IR spectra of the solid surface in the range 4000–300 cm^{-1}. FTIR analysis of the sorbent surface before and after the sorption reaction has provided information regarding the surface groups that might have participated and also about the surface sites at which sorption might have taken place (Fig. 10). The shift of stretching frequency, corresponding to the presence of –OH groups from 3626 to 3451 cm^{-1} is assigned to the involvement of hydroxyl groups in the fluoride adsorption by ZICNSC.

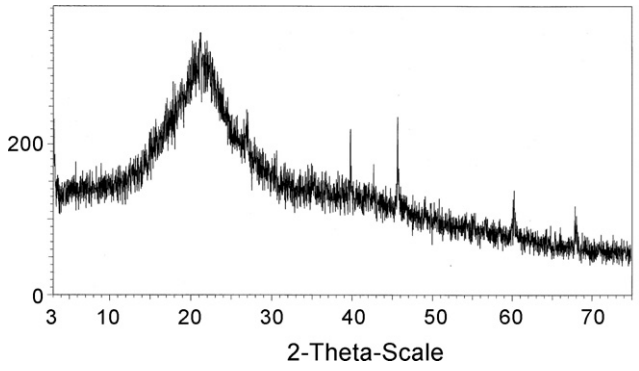

Fig. 8. X-ray diffraction pattern of ZICNSC.

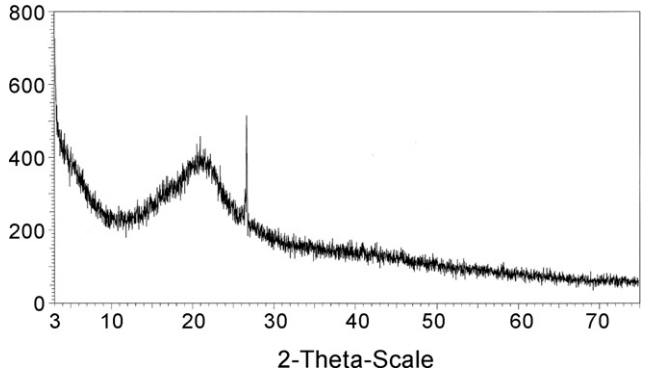

Fig. 9. X-ray diffraction pattern of fluoride adsorbed on ZICNSC.

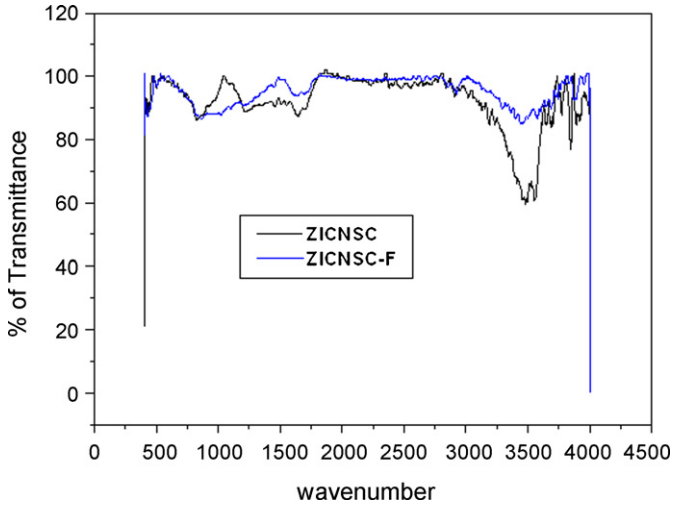

Fig. 10. FTIR spectra of ZICNSC and fluoride treated ZICNSC.

4. Conclusion

In the present study, a zirconium impregnated bioadsorbent was studied for the removal of fluoride ions from aqueous solution. The method is simple and has shown great potential for the removal of fluoride ions. The treatment conditions were optimized: pH value was 7, room temperature and particle size was 53 μm. 80.33% salt rejection has been identified in 3 mg/L of 100 ml fluoride using 1.5 mg dosage of adsorbent. The equilibrium sorption data agree reasonably well for Langmuir isotherm model. Sorption dynamic study revealed that the sorption process followed pseudo-second-order equation; the sorption process was complex, both at the boundary of liquid film and intra-particle diffusion contributed to the rate-determining step. The used adsorbents could be regenerated by 96.2% of 2.5% Sodium hydroxide in 180 min.

Acknowledgement

Financial support for the project by the University Grant Commission (UGC), Government of India, New Delhi under the major research project F. No. 32-296/2006(SR) is gratefully acknowledged.

References

[1] Protection of the Human Environment (PHE), Fluoride in drinking water. WHO, 2001. <http://www.unicef.org/Programme/wes/info/fluor.htm>.
[2] A.K. Susheela, Cited in Prevention and Control of Fluorosis in India, Rajiv National Drinking Water Mission, Ministry of Rural Development, New Delhi, Health Aspect I, 1993.
[3] G. Alagumuthu, M. Rajan, Monitoring of fluoride concentration in ground water of Kadayam block of Tirunelveli district, India, Rasayan J. Chem. 4 (2008) 757–765.
[4] G. Viswanathan, A. Jaswanth, S. Gopalakrishnan, S. Siva ilango, Mapping of fluoride endemic areas and assessment of fluoride exposure, Sci. Total Environ. 407 (5) (2008) 1579–1587.
[5] S.O. Maurice, M. Hitoki, Fluoride removal from water using adsorption technique, Adv. Fluorine Sci. 2 (2006) 1.
[6] M. Tahaikt, R. El Habbani, A. Ait Haddou, I. Achary, Z. Amor, M. Taky, A. Alamib, A. Boughriba, M. Hafsi, A. Elmidaou, Fluoride removal from groundwater by nanofiltration, Desalination 212 (2005) 46–53.
[7] M.A.M. Sahli, S. Annouar, M. Tahaikt, Fluoride removal for underground brackish water by adsorption on the natural chitosan and electrodialysis, Desalination 212 (2007) 37.
[8] E. Erdem, T. Ali, C. Yunus, K. Izzet, Electrodialytic removal of fluoride from water: effects of process parameters and accompanying anions, Sep. Purif. Technol. 64 (2008) 147–153.
[9] A. Tor, Removal of fluoride from water using anion-exchange membrane under Donnan dialysis condition, J. Hazard. Mater. 141 (2007) 814–818.
[10] M. Srimurali, A. Pragathi, J. Karthikeyan, A study on removal of fluorides from drinking water from by adsorption onto low-cost materials, Environ. Pollut. 99 (1998) 285.
[11] Y. Cengeloglu, E. Kir, M. Ersoz, Removal of fluoride from aqueous solution by using red mud, Sep. Purif. Technol. 28 (2002) 81–86.
[12] A. Tor, N. Danaoglu, G. Arslan, Y. Cengeloglu, Removal of fluoride from water by using granular red mud: batch and column studies, J. Hazard. Mater. 164 (2009) 271–278.
[13] R. Sai sathish, N.S.R. Raju, G.S. Raju, G. Nageswara Rao, K. Anil Kumar, C. Janardhana, Equilibrium and kinetics studies for fluoride adsorption from water on zirconium impregnated coconut shell carbon, Sep. Sci Technol. 42 (2007) 769–788.
[14] Ali Tor, Removal of fluoride from an aqueous solution by using montmorillonite, Desalination 201 (2006) 267–276.
[15] C.R. Nagendra Rao, J. Bunch Martin, V. Madha Suresh, T. Vasantha Kumaran (Eds.), Proceedings of the Third International Conference on Environment and Health, Chennai, India, 2003, pp. 386–399.
[16] F. Luo, K. Inoue, The removal of fluoride ion by using metal (III)—loaded Amberlite resins, Solv. Extr. Ion Exch. 22 (2004) 305.
[17] P.S. Ricardo, A.A.X. Santiago, C.A.A. Gadelha, J.B. Cajazeiras, B.S. Cavada, J.L. Martins, T.M. Oliveira, G.A. Bezerra, R.P. Santos, V.N. Freire, Production and characterization of the cashew (*Anacardium occidentale* L.) peduncle bagasse ashes, J. Food Eng. 79 (2007) 1432–1437.
[18] D. Seethapathirao, Defluoridation water using sulphated coconut shell carbon, Indian J. Environ. Health 64 (1964) 11–12.
[19] H.C. Loh, S.M. Ng, M. Ahmad, Accurate zirconium detecting at visible wave length using artificial neural network, Anal. Lett. 38 (2005) 1305–1316.
[20] J.H. Kennedy, Analytical Chemistry Principles, 2nd ed., W.B. Saunder, New York, 1990.
[21] American Public Health Association, Standard Methods for the Examination of Water and Waste Water, Washington, DC, 2005.
[22] M.V. Lopez-Ramon, F. Stoeckli, C. Moreno-Castilla, F. Carrasco-Marin, On the characterization of acidic and basic surface sites on carbons by various techniques, Carbon 37 (1999) 1215–1221.
[23] G. Karthikeyan, S. Siva Ilango, Fluoride sorption using Morringa Indica-based activated carbon, Iran J. Environ. Health Sci. Eng. 4 (2007) 21–28.
[24] G. Karthikeyan, A. Shanmuga Sundarraj, S. Meenakshi, K.P. Elango, Adsorption dynamics and the effect of temperature of fluoride at alumina solution interface, J. Indian Chem. Soc. 81 (2004) 461–466.
[25] I. Langmuir, The constitution and fundamental properties of solids and liquids, J. Am. Chem. Soc. 38 (1916) 2221–2295.
[26] H.M.F. Freundlich, Uber die adsorption in losungen, Z. Phys. Chem. 57A (1906) 385–470.
[27] O. Redlich, D.L. Peterson, A useful adsorption isotherm, J. Phys. Chem. 63 (1959) 1054.
[28] T.W. Weber, R.K. Chakravorti, Pore and solid diffusion models for fixed bed adsorbers, J. Am. Inst. Chem. Eng. 20 (1974) 228–238.
[29] Y.S. Ho, Selection of optimum sorption isotherm, Carbon 42 (2004) 2115–2116.
[30] A.A. Khan, R.P. Singh, Adsorption thermodynamics of carbon Sn(IV) arsenosilicate in H^+, Na^+, and Ca^+ forms, Colloids Surf. 24 (1987) 33–42.
[31] M. Horsfall, A. Spiff, Effect of temperature on the sorption of Pb^{2+} and Cd^{2+} from aqueous solution by caladium bicolor (wild cocoyam) biomass, Electron. J. Biotechnol. 8 (2005) 162–169.
[32] E. Eren, Removal of copper ions by modified Unye clay, Turkey, J. Hazard. Mater. 159 (2008) 235–244.
[33] Y.S. Ho, J.C.Y. Ng, G. McKay, Kinetics of pollutant sorption by biosorbents: review, Sep. Purif. Methods 29 (2000) 189–232.
[34] S. Lagergren, K. Sven, Zur theorie der sogenannten adsorption gelöster stoffe, Vetenskapsakad Handl. 24 (1898) 1–39.
[35] Y.S. Ho, Second order kinetic model for the sorption of cadmium onto tree fern: a comparison of linear and non linear methods, Water Res. 40 (2006) 119–125.
[36] C. Sairam Sundaram, N. Viswanathan, S. Meenakshi, Uptake of fluoride by nano-hydroxyapatite/chitosan, a bioinorganic composite, Bioresour. Technol. 99 (2008) 8226–8230.
[37] D. Wankasi, M. Horsfall, A.I. Spiff, Retention of Pb(II) ion from aqueous solution by nipah palm (nypa fruticans wurmb) petiole biomass, J. Chil. Chem. Soc. 50 (2005) 691–696.
[38] S. Meenakshi, N.J. Viswanathan, Identification of selective ion exchange resin for fluoride sorption, J. Colloid Interf. Sci. 308 (2007) 438–450.